Journal of Sound and Vibration (1998) **217**(3), 405–417
Article No. sv981773

INFLUENCE OF SHAPE AND ABSORBING SURFACE—A NUMERICAL STUDY OF RAILWAY NOISE BARRIERS

P. A. Morgan and D. C. Hothersall

Department of Civil & Environmental Engineering, University of Bradford, Bradford BD7 1DP, England

and

S. N. Chandler-Wilde

Department of Mathematics and Statistics, Brunel University, Uxbridge UB8 3PH, England

(*Received* 28 *November* 1997)

Results are presented of a study of the performance of various track-side railway noise barriers, determined by using a two-dimensional numerical boundary element model. The basic model uses monopole sources and has been adapted to allow the sources to exhibit dipole-type radiation characteristics. A comparison of boundary element predictions of the performance of simple barriers and vehicle shapes is made with results obtained by using the standard U.K. prediction method. The results obtained from the numerical model indicate that modifying the source to exhibit dipole characteristics becomes more significant as the height of the barrier increases, and suggest that for any particular shape, absorbent barriers provide much better screening efficiency than the rigid equivalent. The cross-section of the rolling stock significantly affects the performance of rigid barriers. If the position of the upper edge is fixed, the results suggest that simple absorptive barriers provide more effective screening than tilted barriers. The addition of multiple edges to a barrier provides additional insertion loss without any increase in barrier height.

1. INTRODUCTION

Noise nuisance from railways has become a major concern particularly near lines which carry heavy traffic at high speeds. Noise barriers are commonly used to alleviate the problem. A range of experimental and theoretical studies have been reported on the efficiency of plane screens and other forms of noise barrier in attenuating railway noise [1–6]. In this paper results are presented of a study of the performance of various forms of track-side noise barrier, determined by using a numerical model based on the solution of a two-dimensional boundary integral equation [7]. The model has been adapted to allow for the simulation of dipole-type sources. Use of the model enables the effects of many factors which affect the performance of noise barriers to be investigated in a controlled manner.

0022–460X/98/430405 + 13 $30.00/0

A comparison is carried out of the performance of simple barriers and vehicle shapes, calculated using monopole and dipole sources, with results obtained by using the standard U.K. prediction method, the *Calculation of Railway Noise* [8]. Results are presented showing the effects of the cross-sectional profile of the rolling stock. For a cross-section representative of high speed trains, calculations have been carried out on a wide range of barrier profiles to establish the effect of barrier shape on screening performance. The barrier position relative to the track has been chosen by using an appropriate structure gauge.

2. SELECTION OF SOURCE CHARACTERISTICS

2.1. SOURCE POSITION

Three main forms of noise generation occur on railway trains. These are from the interaction and vibration of the rails and wheels, aerodynamically induced sound from the vehicle body and pantograph, and power unit noise (see, e.g., reference [9]).

Noise from locomotives is less dependent on movement than that from other sources and the array of individual source components varies with the type of vehicle. For high speed trains, which are of primary concern, the power units are located at the ends of the train. The aim here is to predict levels which could be expected when the centre of the train passes the observation point, when power unit sources will have little contribution to the overall level, particularly for receiver positions relatively close to the track.

King [10] observed that aerodynamic sound sources on a high speed train include pantographs and other roof-mounted equipment, bogie units and the "cut-out" areas of the body shell into which these are mounted, and detached flow at the head of the leading car. At high speeds, the latter often produces the strongest aerodynamic source, followed by vortex shedding from pantographs. For the most part, such sources have been shown [11] to be unimportant at speeds below 240 km/h although experimental results from studies of the French TGV-Atlantique [12] have suggested that this limit is actually as high as 300 km/h. Aerodynamic noise tends to increase more dramatically with speed than wheel/rail noise. Measurements performed by Hölzl *et al*. [13] indicated that for high speed trains the noise levels resulting from pantograph noise and wheel/rail noise on the front and rear power cars are similar. The sound propagating from the majority of aerodynamic sources on the upper half of the train body, the pantograph and also the locomotive exhaust outlets will be unobstructed by a typical low barrier of approximately 2 m in height. The direct propagation of sound from these sources should thus be considered separately. Barriers 5–6 m in height would be necessary to shield the surroundings from these sources. In the region of the rails and wheels noise arising from vibration and interaction of these elements is significantly shielded by low barriers. The purpose of this investigation is to examine the attenuation of noise produced in this region.

Van Leeuwen [14] conducted a survey of various prediction models used to determine the effects of track-side noise barriers and found that from the 14 models studied, 9 different source positions were used. These were located predominantly

above either the centreline of the nearest track or the nearside rail and all at heights of $<1{\cdot}0$ m above the trackbed.

In theoretical calculations Ughi *et al*. [15] used a source spectrum composed of wheel/rail noise, pantograph and aerodynamic noise but maintained the source position at the railhead. A source position at the railhead was used in this investigation.

2.2. SOURCE SPECTRUM

There are considerable difficulties in establishing a typical source spectrum for a train. Apart from individual variations between vehicles, the distribution of the sources is diverse and the relative contributions to the overall noise levels vary with speed.

Hemsworth [16] presented wheel/rail noise spectra for several vehicle types, using different wheel diameters and either tread or disc-braked wheels. These included British Rail Mk II and Mk III carriages fitted with tread-brakes and disc-brakes respectively. The A-weighted spectrum for the Mk III carriages is shown in Figure 1. The train speed for this particular data was 160 km/h and the measurement position was 25 m from the nearside track. Figure 1 also shows bypass spectra established during other studies. These have all been adapted to values equivalent to a measurement position of 25 m from the nearside track and are as follows.

Houtave [17]. Measured data from studies of the TGV-Atlantique to investigate the performance of noise barrier systems (rolling stock, TGV-Atlantique; train speed, 300 km/h, original measurement position was at 25 m).

Van Der Toorn [18]. Measured data from studies of the TGV-Atlantique to identify the vertical distribution and strength of acoustic sources (rolling stock,

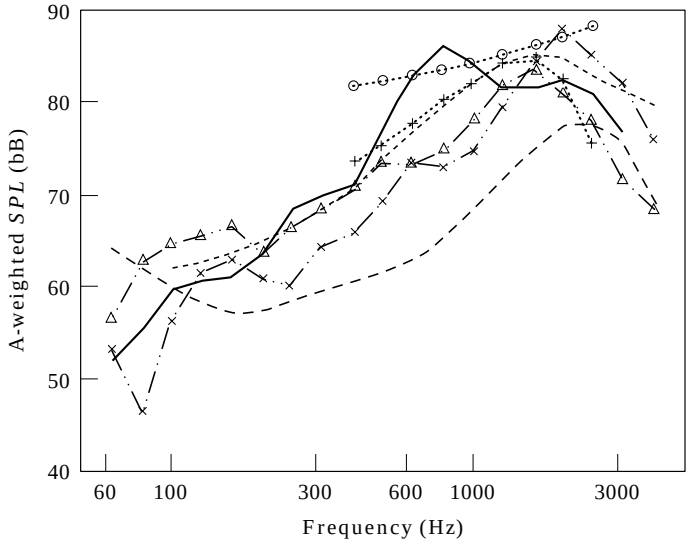

Figure 1. 1/3 octave band A-weighted bypass spectra for different rolling stock. Adjusted for measurement position at 25 m from the nearside track. ——, Hemsworth; – – –, Houtave; +, Van Der Toorn (1); ○, Van Der Toorn (2); ×, Feldmann (1); △, Feldmann (2); — — —, Ughi.

TGV-Atlantique; train speeds, 200 km/h (1) and 300 km/h (2); original measurement position was at 25 m).

Feldmann [19]. Measured data for coaches with different wheel types from a study of the noise behaviour of wheel/rail-systems (rolling stock, carriages with absorber rim damping (1) and sandwich disk damping (2); train speed, 200 km/h; original measurement position was at 3 m).

Ughi [15]. Measured data from a study into the combined effectiveness of different height noise barriers. This spectrum is a combination of wheel/rail, pantograph and aerodynamic noise (rolling stock, ETR 500; train speed, 250 km/h; original measurement position is not specified).

Although there is considerable variation in the results shown in Figure 1 the general trend is similar, with a peak in the spectrum at approximately 1–2 kHz. The source spectrum used in the investigation was that of Hemsworth for British Rail Mk III disc-braked rolling stock.

2.3. SOURCE RADIATION CHARACTERISTICS

Wheel/rail noise is commonly modelled by a line of incoherent dipole sources. This approximation gives good agreement with measured data [20]. Hohenwarter [21] conducted measurements at short distances for a selection of different trains and speeds and found that in most cases electrically hauled trains radiate sound with dipole source characteristics. The ÖAL model [22] uses a combination of dipole and monopole sources, with the ratio 15% monopole and 85% dipole type radiation.

3. THE BOUNDARY ELEMENT MODEL

The approach adopted in this study is to solve accurately the governing wave equation by using the boundary element method which allows complete flexibility in the specification of noise barrier design, shape of rolling stock, and distribution and type of ground surface and absorbent barrier elements. To obtain a computationally manageable problem, the noise barriers and rolling stock are approximated as infinitely long and of uniform cross-section and acoustical properties along their length. The excitation is modelled by coherent line monopole and dipole sources. Then the mathematical problem reduces to solving the two-dimensional Helmholtz equation in the plane perpendicular to the track and noise barriers. In this plane Cartesian co-ordinates Oxy are adopted, with the y-axis vertically upwards. The axes are chosen so that the boundary (ground surface, noise barriers, rolling stock, etc.) lies entirely on or above the line $y = 0$ and, in the cases treated, the ground surface coincides with the line $y = 0$. The boundary is assumed locally reacting and $\beta(\mathbf{r}_s)$ denotes the surface admittance relative to air at a point $\mathbf{r}_s = (x_s, y_s)$ on the boundary. It is also assumed that, for some constant value β_c, $\beta(\mathbf{r}_s) = \beta_c$ at points on the boundary sufficiently far from the tracks. γ denotes those parts of the boundary on which $\beta \neq \beta_c$ or which lie above the line $y = 0$.

The numerical procedure treats the above problem as a perturbation of the case in which the boundary is coincident with the line $y = 0$ and $\beta \equiv \beta_c$. In this simple

case the propagation problem can be solved exactly. Let $G_{\beta_c}(\mathbf{r}, \mathbf{r}_0)$ denote the Green's function for this problem: i.e., $G_{\beta_c}(\mathbf{r}, \mathbf{r}_0)$ denotes the acoustic pressure at $\mathbf{r}$ when a unit strength monopole source is located at $\mathbf{r}_0$ above a flat homogeneous plane of admittance β_c. Expressions and efficient numerical methods for the evaluation of this Green's function are given in reference [23].

The boundary element method is a numerical method applied to the reformulation of the Helmholtz equation as a boundary integral equation. In this study the integral equation employed [7, 24] is

$$\varepsilon(\mathbf{r})p(\mathbf{r}) = p_0(\mathbf{r}) + \int_\gamma \left(\frac{\partial G_{\beta c}(\mathbf{r}, \mathbf{r}_s)}{\partial n(\mathbf{r}_s)} - \mathrm{i}k\beta(\mathbf{r}_s) G_{\beta c}(\mathbf{r}, \mathbf{r}_s) \right) p(\mathbf{r}_s)\, \mathrm{d}s(\mathbf{r}_s), \tag{1}$$

this equation holding for points $\mathbf{r} = (x, y)$ on or above the boundary, where k is the wavenumber, $p(\mathbf{r})$ denotes the pressure at $\mathbf{r}$ and $p_0(\mathbf{r})$ the pressure that would be measured if the boundary were flat, coinciding with the line $y = 0$, and had constant admittance β_c. For points $\mathbf{r} = (x, y)$ on the boundary, $\varepsilon(\mathbf{r}) = \Omega(\mathbf{r})/(2\pi)$ if $y > 0$, $= \Omega(\mathbf{r})/\pi$ if $y = 0$, where $\Omega(\mathbf{r})$ is the corner angle at $\mathbf{r}$ ($= \pi$ if $\mathbf{r}$ is not a corner). $\varepsilon(\mathbf{r}) = 1$ at points above the boundary. Equation (1) is solved by the piecewise constant collocation boundary element method described in references [7, 25].

For the purpose of this study, the boundary element method is implemented using two sources for each track, located at the railhead and exhibiting either monopole or dipole type radiation characteristics. A separate simulation is made for each source position and the resulting predicted noise levels are added logarithmically.

For a monopole source located at $\mathbf{r}_0$, $p_0(\mathbf{r}) = G_{\beta c}(\mathbf{r}, \mathbf{r}_0)$. A dipole source is two coincident monopole sources. That is, for a dipole source,

$$p_0(\mathbf{r}) = \lim_{h \to 0} \left[\frac{G_{\beta c}(\mathbf{r}, \mathbf{r}_0 + h\mathbf{u}) - G_{\beta c}(\mathbf{r}, \mathbf{r}_0)}{h} \right] = \mathbf{u} \cdot \nabla_{\mathbf{r}_0} G_{\beta_c}(\mathbf{r}, \mathbf{r}_0)$$

$$= u_x \frac{\partial}{\partial x_0} G_{\beta_c}(\mathbf{r}, \mathbf{r}_0) + u_y \frac{\partial}{\partial y_0} G_{\beta_c}(\mathbf{r}, \mathbf{r}_0), \tag{2}$$

where $\mathbf{u} = (u_x, u_y)$ is a unit vector along the axis of the dipole (i.e., the axis of maximum emission). In the simulations carried out it is assumed, as in reference [20], that $\mathbf{u} = (1, 0)$ is in the horizontal direction. Expressions and efficient numerical calculation procedures for $\partial G_{\beta_c}(\mathbf{r}, \mathbf{r}_0)/\partial x_0$ and $\partial G_{\beta c}(\mathbf{r}, \mathbf{r}_0)/\partial y_0$ are given in reference [23].

4. METHOD AND COMPARISON WITH OTHER PREDICTION METHODS

The cross-section of the track, rolling stock, ballast and sound sources is shown in Figure 2, together with a noise barrier situated at one side of the track. This is a multiple edge barrier configuration [26], achieved by fitting two extra panels to a plane screen, which is discussed later. The ground is flat and the non-rigid

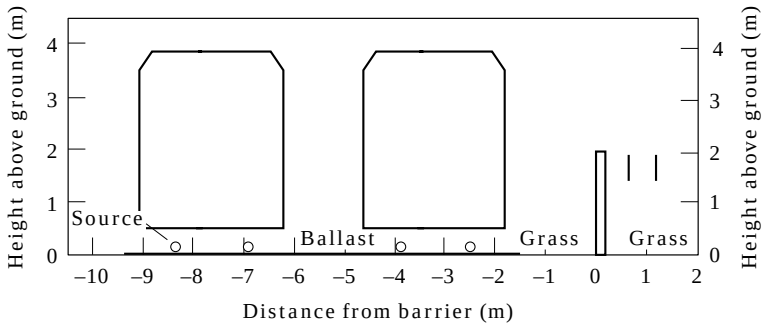

Figure 2. Basic railway cross-section.

surfaces, namely the ballast, grass and absorbing barrier faces, are assumed to consist of a homogeneous porous layer with a rigid backing. The acoustical properties of the porous layer are given by the four-parameter model of Attenborough [27, 28], with use of the parameter values given in Table 1. Type 1 ballast is equivalent to pea-gravel. Type 2 ballast is based upon measurements carried out as part of a study into noise barriers for the TGV [17]. For these preliminary tests, Type 1 ballast is assumed. All other surfaces are assumed rigid, with zero admittance. Receiver positions are located at distances of 20, 40 and 80 m on the far side of the barrier and at heights of 1·5 and 4·5 m. A source is located at each railhead. The source spectrum used is that of Hemsworth for British Rail Mk III disc-braked rolling stock [16] as shown in Figure 1.

Several different configurations of plane screen of different heights were considered which are described in Table 2. For the absorbing barrier case, only the traffic-facing side of the barrier was treated. Insertion losses were calculated at 1/9th octave band centre frequencies and the results combined to obtain a broad band insertion loss. Results for carriages on the nearside and farside tracks were considered separately. Results were calculated by using the boundary element method, for both monopole and dipole sources, and the standard U.K. prediction model, *Calculation of Railway Noise* (CRN) [8].

The insertion losses for the rigid barrier as calculated by using the boundary element method are small for both monopole and dipole sources, not exceeding

TABLE 1

Parameter values used in the impedance model

Surface type	Flow resistivity σ (Ns m^{-4})	Porosity Ω	Tortuosity q	Layer depth d (m)	Pore shape factor s_p
Grass	125 000	0·50	1·67	∞	0·5
Ballast, Type 1	9570	0·40	1·54	0·5	0·4
Ballast, Type 2	180 000	0·40	2·30	∞	0·5
Absorbing barrier	6300	0·90	1·50	0·13	0·5

TABLE 2

Comparison of broad band insertion losses (dB)

Barrier type	Model	Nearside track			Farside track		
		1·5 20·0 (m)	1·5 40·0 (m)	1·5 80·0 (m)	1·5 20·0 (m)	1·5 40·0 (m)	1·5 80·0 (m)
1·5 m rigid	Monopole	3·7	0·0	−4·0	3·3	−0·7	−4·1
	Dipole	3·9	0·3	−3·8	3·4	−0·7	−4·1
	CRN	9·9	9·4	8·7	6·4	5·9	5·3
1·5 m absorbing	Monopole	12·7	9·5	6·2	6·9	3·4	0·7
	Dipole	13·3	10·0	6·9	7·1	3·6	0·8
	CRN	14·3	13·8	13·1	9·6	9·2	8·5
2·0 m absorbing	Monopole	15·6	11·7	8·0	9·6	6·3	2·6
	Dipole	16·2	12·5	8·7	10·0	6·4	2·6
	CRN	16·3	15·7	14·9	11·9	11·2	10·4

4 dB. The introduction of an absorbing surface onto the track-facing side of the barrier significantly improves performance by reducing multiple reflections. Increasing the height of the absorbing barrier further improves performance at all positions. The differences between the monopole and dipole results increases with increasing barrier height, as would be expected from consideration of the emission characteristics.

For the rigid barrier, the boundary element results are very much smaller than those predicted by CRN. This may be because the boundary element method over-estimates the effect of multiple reflections between parallel surfaces due to the perfect geometry of the model and the exactly parallel faces of the rolling stock and barrier. There is good agreement between results from CRN and the boundary element model for the absorbing barriers and the close receiver positions. At larger distances the differences are attributable to ground attenuation which is always considered in the boundary element model. In CRN the gound effect can never exceed 4 dB and is assumed zero when the barrier is present.

Table 3 presents the results from the numerical model when using a dipole source for various plane barrier arrangements and the multiple edge barrier configuration shown in Figure 2. The results suggest that inclusion of the additional panels is equivalent to increasing the height of the plane absorbing barrier by at least 0·5 m.

5. THE EFFECT OF CARRIAGE SHAPE UPON BARRIER PERFORMANCE

To investigate the effect of the carriage shape upon barrier performance, calculations were carried out for a complex cross-section characteristic of high speed trains as shown in Figure 3. This cross-section is based upon British Rail Mk IV carriages and is similar to the profile of TGV rolling stock which is also shown in Figure 3. The barrier position was determined by using standard

TABLE 3

Broad band insertion losses (dB) for various barrier configurations

Barrier type	Nearside track			Farside track		
	1·5 20·0 (m)	1·5 40·0 (m)	1·5 80·0 (m)	1·5 20·0 (m)	1·5 40·0 (m)	1·5 80·0 (m)
1·5 m rigid	3·9	0·3	−3·8	3·4	−0·7	−4·1
1·5 m absorbing	13·3	10·0	6·9	7·1	3·6	0·8
1·5 m absorbing, and RTB panels	15·4	12·3	9·3	9·7	6·1	3·1
2·0 m absorbing	16·2	12·5	8·7	10·0	6·4	2·6
2·0 m absorbing and RTB panels	19·0	14·9	11·1	12·7	8·6	5·0
3·0 m absorbing	18·9	16·3	10·4	13·2	8·3	4·6
3·0 m absorbing and RTB panels	21·2	17·3	13·2	16·4	11·4	6·9

structure gauges [29] and corresponded to the position of overhead cable masts. The impedance characteristics used for the ballast were those given for Type 2 in Table 1. Carriages on the nearside track were considered with a dipole source at each railhead. Results are presented in Table 4, in terms of the mean insertion loss over the 6 measurement positions described previously.

For the case of the rigid barrier, there is a significant improvement in barrier screening when using the complex cross-section, an average of almost 7·5 dB. As already observed, the low values for the simple cross-section are due in part to the perfect geometry of the model. However, the angle of the lower surfaces on the complex cross-section suggests that reflected sound is directed back towards the ground between the train and the barrier, whilst the upper surfaces help direct sound above the receiver positions which have been used.

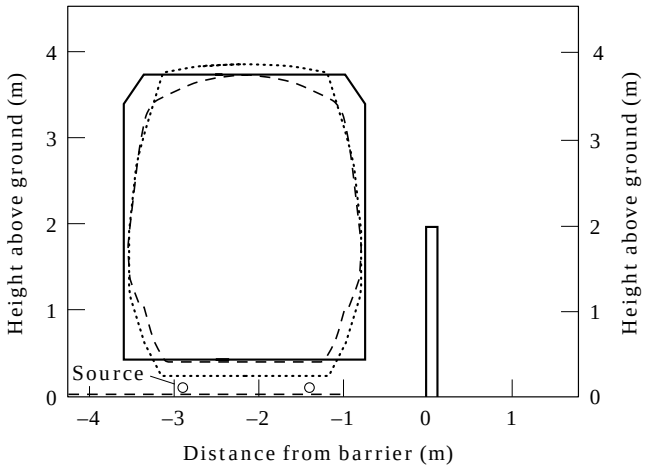

Figure 3. Cross-section for comparison of carriage shapes. — —, Simple; – – –, BR Mk IV; · · · · · , TGV

TABLE 4

Comparison of average insertion losses (dB) for different carriage profiles

Cross-section type	Average insertion loss (dB)	
	Rigid barrier	Non-rigid barrier
Simple	4·1	18·5
Complex	11·4	17·4

Introducing an absorbing surface onto the track-facing side of the barrier reduces the benefits of these inclined rigid-surfaces, leading to a similar degree of screening for the two carriage cross-sections.

6. THE EFFECT OF BARRIER SHAPE UPON SCREENING PERFORMANCE

To investigate the effect of the shape of the noise barrier upon the screening performance, the same basic geometry and sources were adopted as in section 5. The barrier height was 2·0 m. Figure 4 shows the position of five of the different barrier profiles which were studied. The positions were chosen such that no barrier surface fell within the structure gauge. The top edge of the vertical barriers and those inclined towards the track were coincident.

Figure 5 shows the individual barrier arrangements together with the corresponding mean insertion loss over the six measurement positions. In the case of absorbent barriers, the whole track-facing side was treated except in case (d) where the treatment was applied to the upper 0·75 m. "R" denotes the result for a rigid barrier and "A" the absorbing case.

Consider first the rigid barriers [Figures 5(a), (c) and (f)]. The mean insertion loss is in the range 7·1–13·5 dB. Of the three designs, the parabolic form, (c), is

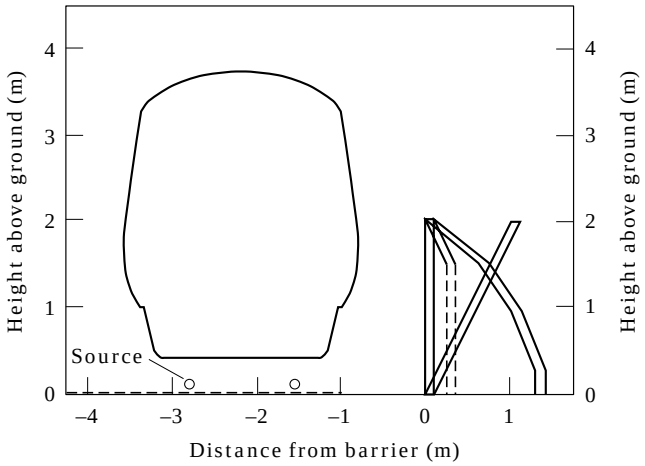

Figure 4. Cross-section for comparison of barrier shapes.

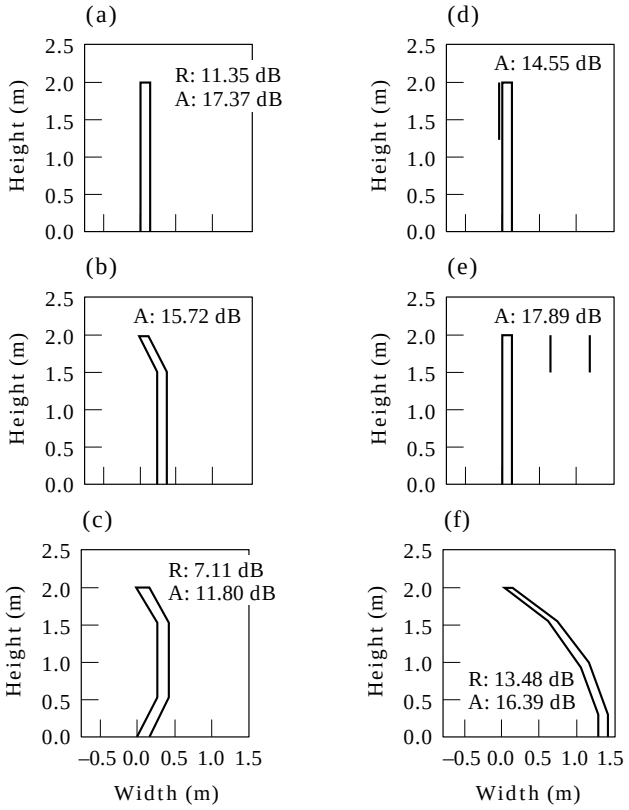

Figure 5. Average insertion losses for the barrier arrangements tested. R = rigid; A = absorbing.

the least efficient. The reason for this may be that the outward sloping lower section of the parabolic profile is reflecting sound upwards and reducing the benefits of profiling the carriage sides. The screen sloping towards the carriage, (f), is more efficient than the plane screen when their upper edges are coincident.

For those barriers with absorbent surfaces, the mean insertion loss is in the range 11·8–17·9 dB. As for the rigid case, barrier (c) produces the lowest value of mean insertion loss. The most efficient single barrier is the plane screen (a). Other designs produce very similar mean insertion losses between these values, as was observed by Van Tol [6]. In assessing the relative efficiency in these cases it must be remembered that the performance will be affected by the criteria used for the relative positions of the upper edges. In this investigation the position of the upper edges are coincident. Other studies [4, 5], in which the feet of the barriers are coincident, report that screens inclined towards the track are the most effective. For the partially absorbing barrier, (e), the mean *IL* is midway between that achieved using either a fully rigid or fully absorbing barrier. In this instance, screening will be improved by increasing the proportion of the barrier surface which is absorbent.

Enhanced screening can be achieved by incorporating multiple edge devices, as was observed by Rudolphi and Åkerlöf [3]. For the complex train cross-section, the insertion loss of the multiple edge device is approximately 0·5 dB greater

than that for the plane absorptive barrier. This is not as significant as was observed during the preliminary tests with a simple cross-section, where the improvement was equivalent to a 0·5 m increase in barrier height.

7. CONCLUSIONS

The boundary element numerical model is a useful tool for investigating the relative efficiency of various forms of track-side noise barrier for railways. The results of the two-dimensional model can be interpreted in three dimensions as equivalent to those for a coherent line source of sound. The results are expected to be representative of levels obtained when the centre of the train passes the observation point.

Sources at the railhead have been used which are appropriate for a variety of sources below the level of the upper edge of the noise barriers. Aerodynamic and power unit noise above the barrier will not be attenuated and have not been considered.

The difference in barrier insertion loss resulting from assuming monopole and dipole source characteristics is quite small, but becomes more important as the height of the barrier increases.

The results obtained by using the numerical model suggest that for any particular shape, an absorbent barrier provides much better screening efficiency than the rigid equivalent. The cross-section of the rolling stock significantly affects the performance of rigid barriers. The screening efficiency of such barriers is poor when the sides of the rolling stock are vertical. However an average improvement in insertion loss of up to 7·5 dB for a 2 m high barrier results when the upper and lower surfaces of the vehicle sides are inclined; this helps to redirect reflected sound either towards the trackbed or upwards. Such profiles are commonly used, particularly on high speed trains.

If the position of the upper edge is fixed, the results suggest that vertical absorptive barriers provide more effective screening than those tilted towards the track, since the benefits of using profiled rolling stock are eliminated. The addition of multiple edges to a barrier provides additional insertion loss of up to 3·0 dB without any increase in height for carriages with vertical sides. The average improvement is 0·5 dB for profiled rolling stock.

REFERENCES

1. Y. Hidaka, H. Tachibana, Y. Matsui and R. Kaneko 1995 *Proceedings of Inter-Noise* '85. Measurement of sound radiation from Shinkansen train by sound intensity method. 215–218.
2. C. J. C. Jones, A. E. J. Hardy, R. R. K. Jones and A. Wang 1996 *Journal of Sound and Vibration* **193**, 427–431. Bogie shrouds and low track-side barriers for the control of railway vehicle rolling noise.
3. E. Rudolphi and L. Åkerlöf 1996 *Proceedings of Inter-Noise* '96. Full scale tests on the design of railway noise barriers. 799–802.

4. P. HOUTAVE and J.-P. CLAIRBOIS 1997 *Proceedings of Inter-Noise* '97. Specific designs of noise barriers for trains. Part I: Theoretical study of forms and materials. 421–424.
5. J.-P. CLAIRBOIS, P. HOUTAVE and N. NICOLAS 1997 *Proceedings of Inter-Noise* '97. Specific designs of noise barriers for trains. Part II: *In-situ* verification of effectiveness. 425–428.
6. P. F. VAN TOL 1997 *Proceedings of Inter-Noise* '97. An array measurement technique applied to high speed train noise barriers. 429–432.
7. D. C. HOTHERSALL, S. N. CHANDLER-WILDE and N. M. HAJMIRZAE 1991 *Journal of Sound and Vibration* **146**, 303–322. Efficiency of single noise barriers.
8. DEPARTMENT OF TRANSPORT 1995 *Calculation of Railway Noise*. London: HMSO.
9. C. STANWORTH 1987 in *Transportation Noise Reference Book* (P. M. Nelson, editor). London: Butterworth. Sources of railway noise.
10. W. F. KING III 1996 *Journal of Sound and Vibration* **193**, 349–358. A précis of developments in the aeroacoustics of fast trains.
11. W. F. KING III 1977 *Journal of Sound and Vibration* **54**, 361–378. On the role of aerodynamically generated sound in determining the radiated noise levels of high speed trains.
12. B. MAUCLAIRE 1990 *Proceedings of Inter-Noise* '90. Noise generation by high speed trains. New information acquired by SNCF in the field of acoustics owing to the high speed test program. 371–374.
13. G. HÖLZL, P. FODIMAN, K.-P. SCHMITZ, M. A. PALLAS and B. BARSIKOW 1994 *Proceedings of Inter-Noise* '94. Deufrako-2: localised sound sources on the high-speed vehicles ICE, TGV-A and TR 07. 193–198.
14. J. J. A. VAN LEEUWEN 1996 *Journal of Sound and Vibration* **193**, 269–276. Noise prediction models to determine the effect of barriers placed alongside railway lines.
15. S. UGHI, F. ARTOM, S. CINGOLANI and L. ASTE 1995 *Proceedings of Inter-Noise* '95. Behaviour of normal height sound barriers combined with low barriers at minimum distance from the railway tracks. 377–380.
16. B. HEMSWORTH 1987 in *Transportation Noise Reference Book* (P. M. Nelson, editor); London: Butterworth. Prediction of train noise.
17. P. HOUTAVE 1997 Acoustical Technologies, Brussels, Belgium. Private communication.
18. J. D. VAN DER TOORN, H. HENDRIKS and T. C. VAN DEN DOOL 1996 *Journal of Sound and Vibration* **193**, 113–121. Measuring TGV source strength with Syntacan.
19. J. FELDMAN 1983 *Journal of Sound and Vibration* **87**, 179–187. The noise behaviour of the wheel/rail-system—some supplementary results.
20. S. PETERS 1974 *Journal of Sound and Vibration* **32**, 87–99. The prediction of railway noise profiles.
21. D. HOHENWARTER 1990 *Journal of Sound and Vibration* **141**, 17–41. Railway noise propagation models.
22. *ÖAL-Richtlinie* No. 30 1990 *Calculation of the sound immission from rail traffic* (in German).
23. S. N. CHANDLER-WILDE and D. C. HOTHERSALL 1995 *Journal of Sound and Vibration* **180**, 705–724. Efficient calculation of the Green's function for acoustic propagation above a homogeneous impedance plane.
24. R. SEZNEC 1980 *Journal of Sound and Vibration* **73**, 195–209. Diffraction of sound around barriers: use of the boundary elements technique.
25. S. N. CHANDLER-WILDE, D. C. HOTHERSALL, D. H. CROMBIE and A. T. PEPLOW 1991 in *Recontres Scientifiques de Cinquantenaire*: *Ondes Acoustiques et Vibratoires*, *Interactions Fluide-Structures Vibrantes*. Publication du Laboratoire de Mécanique et d'Acoustique, C.N.R.S., Marseille, No. 126. Efficiency of an acoustic screen in the presence of an absorbing boundary.
26. D. H. CROMBIE, D. C. HOTHERSALL and S. N. CHANDLER-WILDE 1995 *Applied Acoustics* **44**, 353–367. Multiple-edge noise barriers.

27. K. ATTENBOROUGH 1985 *Journal of Sound and Vibration* **99**, 521–544. Acoustical impedance models for outdoor ground surfaces.
28. K. ATTENBOROUGH and C. HOWARTH 1992 *Proceedings of Inter-Noise* '92. Prediction and measurement of the acoustical performance of porous road surfaces. 223–227.
29. RAILTRACK 1995 *Railway Group Standard GC/RT* 5204, *Structure Gauging and Clearances*.